ELSEVIER

Contents lists available at ScienceDirect

Science of the Total Environment

journal homepage: www.elsevier.com/locate/scitotenv



The effect of biochar nanoparticles on rice plant growth and the uptake of heavy metals: Implications for agronomic benefits and potential risk



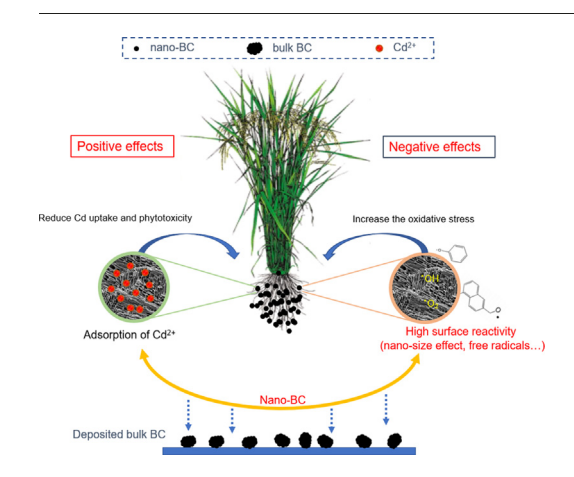
Le Yue ^a, Fei Lian ^{a,b,*}, Yang Han ^b, Qiongli Bao ^b, Zhengyu Wang ^a, Baoshan Xing ^c

- a Institute of Environmental Processes and Pollution Control, School of Environmental and Civil Engineering, Jiangnan University, Wuxi 214122, China
- ^b Agro-Environmental Protection Institute, Ministry of Agriculture, Tianjin 300191, China
- ^c Stockbridge School of Agriculture, University of Massachusetts, Amherst, MA 01003, the, United States

HIGHLIGHTS

- Nano-BC greatly alleviates the phytotoxicity of Cd²⁺ to rice plants.
- Nano-BC differentially affects Cd²⁺ net flux in different zones of root tips.
- Nano-BC increases the antioxidative enzyme activities of rice plants.
- Reduced Cd bioavailability by nano-BC offsets its negative effect on plant growth.
- The potential risks of BC should not overlooked in soil applications.

GRAPHICAL ABSTRACT



ARTICLE INFO

Article history:
Received 29 August 2018
Received in revised form 23 November 2018
Accepted 24 November 2018
Available online 26 November 2018

Editor: Charlotte Poschenrieder

Keywords: Nano-sized biochar Rice plant Phytotoxicity Cadmium Free radical

ABSTRACT

The interaction between biochar nanoparticles (nano-BC) and plant roots in the rhizosphere is largely unknown, although it is crucial for understanding the role of BC in plant growth and bioavailability of pollutants. The effect of nano-BC produced at a series of temperatures (300–600 °C) on alleviating the phytotoxicity of Cd^{2+} to rice plants was investigated from the aspects of biochemical changes and Cd uptake in this study. The kinetics of Cd^{2+} fluxes in different root zones in the presence of nano-BC were also measured using a scanning ion-selective electrode technique. We found that the high-temperature nano-BC could more significantly alleviate the phytotoxicity of Cd^{2+} than the low-temperature and bulk BCs as reflected by the higher increased biomass, root vitality, chlorophyll content, and decreased MDA content as well as relative electrical conductivity of rice plants, which is due to the high adsorption affinity of nano-BC for Cd^{2+} . Also, for the first time we demonstrated that nano-BC could differentially affect the net flux of Cd^{2+} in different zones of the root tips. However, nano-BC (especially that produced at higher temperatures) more significantly increased the contents of antioxidative enzyme activities (e.g., SOD, POD, and CAT) and soluble protein than the treatment only with Cd^{2+} (5.0 mg/L), indicating that nano-BC could induce oxidative stress in the rice plants. These results indicate that nano-BC could greatly reduce the uptake and phytotoxicity of Cd^{2+} , but its potential risk should not be overlooked during the environmental and agricultural applications of biochar.

© 2018 Elsevier B.V. All rights reserved.

^{*} Corresponding author at: Institute of Environmental Processes and Pollution Control, School of Environmental and Civil Engineering, Jiangnan University, Wuxi 214122, China. E-mail address: Flian@jiangnan.edu.cn (F. Lian).

1. Introduction

Biochar (BC) refers to the carbonaceous solid produced by thermochemical pyrolysis of biomass resources under oxygen-limited condition (Pignatello et al., 2006; Qiu et al., 2009). Owing to its unique physicochemical properties (such as abundant functional groups, high surface area and reactivity) and economic availability, BC has been widely used in various environmental and agricultural applications including immobilization of contaminants (Song et al., 2013), carbon sequestration (Singh et al., 2012), and soil modifiers (Silber et al., 2010). BC is a heterogeneous mixture and likely to experience physical disintegration into smaller fragments including colloids (size < 1 µm), nanoparticles (size < 100 nm), and water-soluble fractions because of weathering and aging in the environments (Qu et al., 2016; Spokas et al., 2014). Comparatively, relative to bulk BC, the effect of ultra-fine BC particles on biogeochemical processes (e.g., element cycling, contaminant transport, and plant growth) in environmental media are much less examined.

It is reported that BC fractions below 0.45 µm have higher content of oxygen and polar functional groups, but lower aromaticity and less condensed aromatic clusters compared with bulk BC (Qu et al., 2016). These fine BC particles exhibit high colloidal stability in typical freshwaters due to negatively charged surfaces and small sizes. For example, the critical coagulation concentration of BC nanoparticles (nano-BC) from pecan shells was reported to be 250 mmol/L for Na⁺ and 8.5 mmol/L for Ca²⁺ (Yi et al., 2015). Wang et al. (2012) found that nano-BC had much greater mobility in saturated granular media than BC micrometer particles. These results indicate that nano-BC is active and inclined to transport both laterally and vertically in terrestrial and aquatic ecosystems (Major et al., 2010). Also, it tends to bind with soil organic matter and minerals to form microaggregates via organo-mineral interactions (Weng et al., 2017; Archanjo et al., 2017). It is foreseeable that nano-BC (including its microaggregates) will more easily enter into rhizosphere and contact with plant roots relative to bulk BC. Previous literatures have well demonstrated that BC plays an important role in the immobilization of pollutants, plant growth, and crop yield (Khan et al., 2013; Sun et al., 2014; Van Zwieten et al., 2010). However, some recent studies found that BC could inhibit the germination and growth of plants due to the presence of free radicals (Liao et al., 2014) and/or phytotoxic compounds and heavy metals (Rogovska et al., 2012). This paradox can be better clarified and understood by examining the interaction between nano-BC and plant roots in the rhizosphere, which is one of the most critical zones for plants to communicate with the environment. However, to our knowledge, little effort has been made to systematically assess the possible positive and negative effects of BC on biota development and related mechanisms in the rhizosphere. We hypothesize that the nano-BC attached to root surfaces could reduce the phytotoxicity of heavy metals and their uptake by plants due to the high adsorption capacity of nano-BC; while the nano-BC itself could probably lead to morphological or physiological changes of plants because of its unique properties (such as the presence of free radicals, inherent contaminants, and high redox potential) (Klüpfel et al., 2014).

Therefore, the objective of this study was to systematically assess the role of nano-BC in alleviating the phytotoxicity of heavy metals to rice plants from the aspects of growth, biochemical changes, and heavy metal uptake, and meanwhile to detect the potential risk (if any) of nano-BC to plant growth after its attachment onto root surfaces. The nano-BC in this study was fractionated from rice hull BC prepared under a series of charring temperatures (300–600 °C). The biochemical assays were conducted to determine chlorophyll content and membrane permeability of leaves, root vitality, soluble protein content, as well as antioxidant responses. Cadmium (Cd) was selected as a representative of heavy metals due to its wide presence and frequency being examined in the environmental media (Du et al., 2012). The spatial characteristics and real-time kinetics of Cd transport in rice plant roots with and without the presence of nano-BC were determined

using a non-invasive Cd-selective microelectrode technique. To the best of our knowledge, this is the first study to quantitatively examine the role of nano-BC in decreasing Cd²⁺ flux between roots and surrounding solutions. The result of this study would provide more information regarding the interaction of BC with plant roots in the rhizosphere and its effect on the bioavailability of pollutants.

2. Materials and methods

2.1. Preparation of bulk BC

Rice-hull BC, carbonized at a range of temperatures (300, 400, 500, and 600 °C) for 2 h at an oxygen limited condition, was used as bulk BC particles. Prior to carbonization, the rice hulls were washed with tap water several times and dried at 80 °C for 24 h. The raw material was crushed and passed through a 2.0 mm mesh. The obtained BC was ground, sieved through a 150 μ m mesh, and labeled as B300-B600, respectively.

2.2. Characterization of nano-BC

Nano-BC was fractionated from the bulk BC powders according to the protocol in our recent study (Liu et al., 2018). Briefly, the bulk BC powder was thoroughly mixed with deionized (DI) water and then set quiescently for 2 h. The upper layer of suspension was siphoned off and centrifuged at 10,000 rpm for 30 min. The supernatant was freeze-dried to obtain nano-BC. The obtained samples were referred to as N300-N600, respectively. The stock suspension of nano-BC was prepared by stirring 50 mg nano-BC into 500 mL of 25% nutrient solution (see Section 2.4 for its composition) overnight, and then sonicating thoroughly. The pH of nano-BC suspensions was adjusted to 6.5 with NaOH and HCl.

The samples of N300-N600 and B600 (for comparison) were characterized for their surface elemental composition with a X-ray photoelectron spectrometer (XPS, PHI 5000 VersaProbe, Japan). The crystal structures were observed using X-ray diffraction (XRD, RIGAKV 2500 PC, Japan) with Cu K α as a source of radiation (40 kV, 40 mA, I = 1.5406 Å) over the 2 θ range of 10° to 80°. The surface area, total pore volume, and average pore diameter were measured by N₂ adsorption-desorption at 77 K by an Autosorb-1 gas analyzer (Quantachrome Instruments, USA). Hydrodynamic diameters (D_h) were determined by a dynamic light scattering (DLS) analyzer (90Plus, Brookhaven, USA).

2.3. Electron paramagnetic resonance (EPR) measurements

The nano-BC particles were loaded into quartz capillary tubes for EPR measurements on a Bruker X-band A300-6/1 EPR spectrometer at room temperature (Yang et al., 2016). The EPR spectrometer parameters used for measurements were: modulation frequency of 100 kHz, microwave frequency of 9.86 GHz, microwave power of 0.1 mW, modulation amplitude of 3.00 G, receiver gain of 3.17×10^3 , center field of 3520 G, sweep width of 400 G, resolution of 1024 points, time constant of 20.48 ms, and sweep time of 102.4 s. The relative intensity of radical response was measured as peak-to-peak height.

2.4. Hydroponic culture and treatments

Rice seeds (*Oryza sativa* L.) were provided by Xiangyin Seed Company, Hunan, China. The sterilized (4% NaClO, 15 min) seeds were initially germinated in vermiculite medium and irrigated with distilled water. After germination, the seedlings were irrigated with 25% strength of the following nutrient solution (mmol/L) for two weeks: 89 mg/L Ca(NO₃)₂·4H₂O, 250 mg/L MgSO₄·2H₂O, 49 mg/L (NH₄)₂SO₄, 34 mg/L KH₂PO₄, 30 mg/L FeCl₂, 2.86 mg/L H₃BO₃, 0.22 mg/L ZnSO₄·7H₂O, 1.81 mg/L MnCl₂·2H₂O, 0.08 mg/L CuSO₄·5H₂O, and 0.02 mg/L H₂MoO₄·4H₂O. The pH of the nutrient solution was adjusted

to 6.5 with NaOH and HCl. The seedlings were incubated in a growth chamber, with a 12 h photoperiod, 25/20 °C day/night temperature, and 60% relative humidity. After the appearance of the third leaflet, uniform seedlings were selected, rinsed thoroughly and transferred into a plastic container with DI water. After 24 h, every 10 seedlings were transplanted into a 250 mL brown glass bottle containing a 200 mL suspension of nano-BC (i.e., N300-N600), respectively. Meanwhile, B600 with a same aqueous concentration was selected for comparison to demonstrate the unique role of nano-BC in plant growth, Cd uptake, and physiological responses of rice plants. After that, an aliquot of Cd² stock solution was injected into the suspension to ensure that the final concentration of Cd²⁺ was 5.0 mg/L, at which little severe adverse effect was observed on rice growth in our previous study (Zhao et al., 2017). Vials receiving Cd²⁺ spiked (5.0 mg/L) nutrient solution instead of BC suspensions were used as the control treatment. The exposure experiment lasted for 7 days and the vails were gently stirred every day to ensure the BC particles were well suspended.

2.5. Plant height, dry weight, root morphology, and Cd content

After exposure, the heights of the seedlings were measured and then the rice plants were washed with flowing tap water and DI water several times. The root morphological parameters including accumulative root length, surface area, volume, average diameter, number of root tips and crossings were analyzed with the WinRhizo system v. 4.0b (Regent, Canada). Then, a portion of fresh samples (shoots or roots) was weighed and stored in a refrigerator for the analysis of chlorophyll, membrane permeability of leaves, soluble protein, and antioxidant enzyme activity. Root vitality was also examined. The remaining samples were dried at 80 °C for 24 h and pulverized for the determination of biomass and Cd contents. The Cd levels in the shoots and roots from all treatments were measured using an atomic absorption spectrophotometer (AAS, VarianAA, USA) after HNO₃ digestion.

2.6. Chlorophyll content and membrane permeability of leaves

The contents of chlorophyll-a and -b, and total chlorophyll in fresh leaves, extracted with a mixture of acetone and ethanol, were measured by an UV spectrophotometer (Agilent 8453, USA) at 663 nm and 645 nm, respectively. For the determination of membrane permeability, fresh leaves (0.2 g) were sampled, placed in capped PVP vials containing 10 mL DI water, and rotated (100 rpm) at 25 °C for 24 h. Then, electrical conductivity (L_1) of the bathing solution was determined. After that, the samples were autoclaved at 120 °C for 20 min and electrical conductivity (L_2) was measured again upon equilibration at 25 °C. The electrolyte leakage ratio was defined as L_1/L_2 (%).

2.7. Root vitality and soluble protein content of rice plants

Root vitality of the rice plants was examined with the triphenyl tetrazolium chloride (TTC) method (Lindström and Nyström, 1987). Briefly, 1.0 g of root samples were weighed and added into 10 mL tubes containing 0.4% TTC and 0.06 mmol/L NaHPO₄-KH₂PO₄ (pH 7.0). The samples were incubated at 37 °C for 3.0 h. Extraction of the root samples was conducted in capped tubes with 10 mL methyl alcohol and remained for 24 h. The absorbances were recorded by an UV spectrophotometer at 485 nm.

Soluble protein content was measured according to the Bradford assay (Marion, 1976). Fresh shoots or roots (0.5 g) were homogenized in 10 mL phosphate buffer (pH 7.8) and then centrifuged at 10,000 rpm for 20 min. The protein extract (0.1 mL) was mixed with 0.9 mL tris-HCl buffer solution and 5 mL Coomassie reagent (G-250), shaken well, and equilibrated at room temperature for 2 min. At 595 nm, absorbances were recorded using DI water as a blank. The concentrations of proteins were determined from a standard curve of bovine serum albumin (BSA).

2.8. Antioxidant determination

For the enzyme studies, shoots and roots were separately homogenized, centrifuged, and the extract was analyzed for superoxide dismutase (SOD), peroxidase (POD), and catalase (CAT) as described in previous studies (Rico et al., 2013; Zhang et al., 2014). Briefly, SOD activity was analyzed based on its ability to inhibit the photoreduction of nitro-blue-tetrazolium (NBT); i.e., one unit of SOD activity is defined as the amount of enzyme that causes a 50% decrease of NBT reduction. POD activity was measured at 25 °C by monitoring the increase in absorbance at 470 nm due to guaiacol oxidation. One unit of POD activity is the amount of enzyme leading to an increase in absorbance of 0.01 at 470 nm per minute. CAT activity was determined by monitoring the absorbance decrease at 240 nm due to the degradation of H₂O₂. The lipid peroxidation level in the roots and shoots was determined in terms of Malondialdehyde (MDA, lipid peroxidation product) content, which was measured with the 2-thiobarbituric acid (TBA) method (Shah et al., 2001). A portion of fresh leaves (0.5 g) was ground in the reaction substrate of 0.5% TBA and 10% trichloroacetic acid (TCA) solutions. After heated at 100 °C for 30 min, the mixture was cooled down in an ice bath and centrifuged at 4000 rpm for 10 min. The MDA content was calculated based on the absorbance of the supernatant at 450, 532, and 600 nm, respectively.

2.9. Measurement of Cd^{2+} flux

Cd²+ flux was examined noninvasively using a scanning ion-selective electrode technique (SIET) (SIET system BIO-001A; Younger USA Sci. & Tech. Corp.) at Xu-Yue Sci. & Tech. Co. Ltd. (Beijing, China). The microelectrodes were calibrated in 10, 50 and 100 μ mol/L CdCl² solution before the measurement of net Cd²+ flux based on the standard procedure (Xu-Yue Sci. & Tech. Co. Ltd). Only electrodes with Nernstian slopes in the range of 29 ± 3 mV/decade were used (Sun et al., 2013). Fresh roots of rice plants, rinsed with DI water, immobilized in the measuring solution (5.0 mg/L CdCl², 50 μ mol/L CaCl², pH 5.5), and then equilibrated for 20 min. The Cd²+ fluxes were recorded and lasted for 10 min in the elongation zone, root hair zone, and root cap area, respectively. All experiments were repeated at least three times and their mean values \pm SD are presented. The flux data were calculated using MageFlux, which was developed by the Xu-Yue Sci. & Tech. Co. Ltd.

2.10. Cd²⁺ adsorption experiment

A batch equilibrium method was used to compare the adsorption capacity of nano-sized BC with bulk BC for Cd^{2+} at 25 °C. The stock solution of Cd^{2+} (pH 6.0) was sequentially diluted to seven different concentrations in the range of 12.5–250 mg/L. For bulk BC (i.e., B300-B600), 200 mg of the particle and 20 mL of CdCl_2 solution were added into 40-mL vails. For nano-sized BC (i.e., N300-N600), 3 mL of BC stock suspensions (100 mg/L) and 1 mL of CdCl_2 solution were added into 8-mL vails, where the solid/solution ratio was selected based on our preliminary study. All the vials were shaken for 24 h to reach apparent adsorption equilibrium. Once the solutions were sampled and filtered, the Cd^{2+} concentration in the supernatant were determined by AAS. The adsorption experiment was conducted in duplicate. Control experiments without any adsorbent in the vials were carried out simultaneously. No measurable change in the Cd^{2+} concentrations was observed in the controls.

2.11. Statistical analysis

The data obtained from various morphological and physiological parameters were subjected to one-way analysis of variance (ANOVA). Significant differences among the treatments at p < 0.05 were evaluated by the Tukey-HSD multiple comparisons using SAS software 19.0 (SAS Institute Inc. Cary, NC, USA).

Table 1 Surface elemental composition, BET surface area (N_2 - S_{BET}), total pore volume (V_{tot}), and average pore diameter (D_n) of the nano- and bulk BCs.

ВС	Surface elemental composition (%)				ion (%)	N ₂ -S _{BET}	V _{tot}	$D_{\rm p}$
	C 1s	N 1s	O 1s	Si 2p	(0 + N)/C	(m^2/g)	(cm ³ /g)	(nm)
N300	71.34	2.43	21.65	_	0.338	21.7	0.046	8.39
N400	71.19	3.29	20.34	0.37	0.332	80.1	0.051	5.52
N500	81.25	1.91	14.95	0.97	0.208	90.9	0.013	4.82
N600	80.87	1.27	14.84	1.34	0.199	123.2	0.062	5.94
B600	79.62	1.08	12.08	1.83	0.165	27.1	0.036	5.36

3. Results and discussion

3.1. Characteristics of nano-BC

The $D_{\rm h}$ of nano-BC in the suspension after sonication was measured by DLS (Fig. S1). The average particle size of nano-BC gradually decreased with increasing carbonization temperature, where the $D_{\rm h}$ of N300-N600 was 190 nm, 106 nm, 92 nm, and 59 nm, respectively. Thus, BC particles with smaller size are more easily formed or fractionated at higher charring temperature. Surface elemental composition and pore structure of nano-BC are summarized in Table 1. The surficial C content of nano-BC gradually increased while its polarity index [(O + N)/C] decreased with increasing pyrolytic temperature, suggesting that polar functional groups were significantly reduced and nano-BC became more hydrophobic and aromatic. Besides, the gradually increased content of Si indicates that the mineral elements tend to redistribute from interior to the BC surface at higher temperature (Zhao et al.,

2013). Consistently, more sharp peaks on the X-Ray diffractograms (Fig. S2) were observed for nano-BC, especially more so in the high-temperature ones than the bulk BC, revealing that these minerals were likely to form crystalline substances such as quartz, sylvite, and calcite on the surface of nano-BC. For pore structure of nano-BC, its surface area and pore volume increased from 21.7 to $123.2~\text{m}^2/\text{g}$ and 0.046 to $0.062~\text{cm}^3/\text{g}$, respectively, with charring temperature increasing from 300 to 600~c (Table 1). To distinguish the differences between nano-and bulk-BC, selected properties of B600 were also examined. It is notable that, although surface elemental composition of B600 is comparable to N600, its N₂-S_{BET} and V_{tot} are much lower than those of N600, indicating that nano-BC has more developed pore structure and probably higher adsorption capacity as well as surface reactivity (Pignatello et al., 2017).

3.2. Growth of rice plants

Relative to the treatment with only Cd^{2+} addition (5.0 mg/L), the presence of nano-BC, especially the high-temperature ones, greatly alleviated the adverse effect of Cd^{2+} on the growth of rice plants. As shown in Fig. 1, the biomass dry weight (shoots and roots) and height with the presence of N500 and N600 were significantly higher than those without BC. However, bulk BC (i.e., B600) contributed little to alleviating the negative impact of Cd^{2+} on rice plant growth. Consistently, root morphological parameters such as accumulative root length, number of root tips and crossings are also indicative of the more constructive role of nano-BC (Table 2). The root vitality of rice plants was enhanced by the presence of BC in an order of N600 \approx N500 > N400 > N300 > B600 > control, which is more evident than biomass weight and root

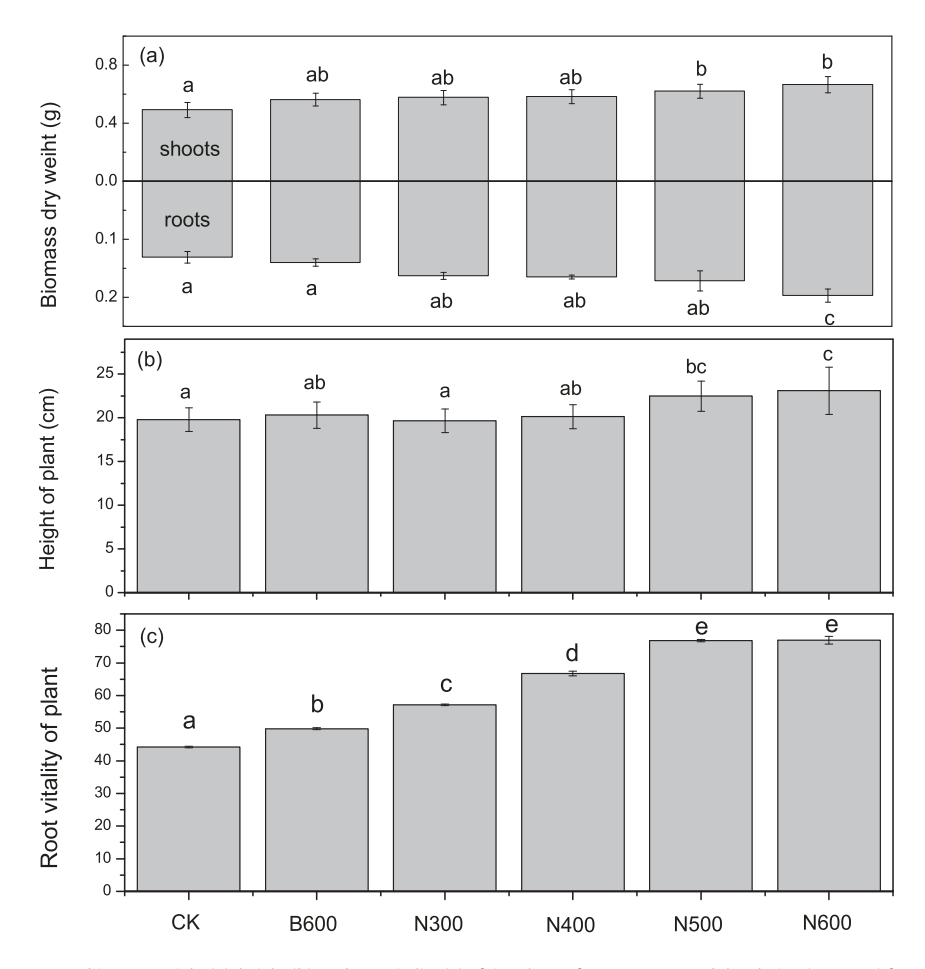


Fig. 1. The effect of bulk- and nano-BCs on biomass weight (a), height (b), and root vitality (c) of rice plants after exposure to $CdCl_2$ solution (5.0 mg/L) for 7 days. Different letters represent different statistical groups suggested by the Tukey-HSD multiple comparisons at p < 0.05.

Table 2 Effect of bulk- and nano-BCs on root parameters of rice plants after exposure to $CdCl_2$ solution (5.0 mg/L) for 7 days. Different letters represent different statistical groups suggested by the Tukey-HSD multiple comparisons at p < 0.05.

treatment	Accumulative root length (cm)	Surface area (cm ²)	Root volume (mm ³)	Average diameter (mm)	Root tips	Root crossings
CK	110.54 ± 23.19 a	6.798 ± 0.88 a	0.031 ± 0.0054 a	0.18 ± 0.014 a	$1145 \pm 332a$	$978\pm187a$
B600	119.65 ± 14.11a	$6.997 \pm 1.42ab$	0.032 ± 0.016 a	0.18 ± 0.004 a	1420 ± 196 ab	$1026\pm233ab$
N300	$123.81 \pm 21.21ab$	8.032 ± 0.61 ab	$0.034 \pm 0.0063a$	0.18 ± 0.015 a	$1446 \pm 502ab$	$1074 \pm 185ab$
N400	$137.36 \pm 30.21ab$	$9.330 \pm 0.77b$	$0.036 \pm 0.0073a$	$0.19 \pm 0.029a$	$1613 \pm 298ab$	$1161 \pm 484ab$
N500	$150.73 \pm 51.39ab$	$8.185 \pm 2.24ab$	$0.038 \pm 0.0033a$	0.20 ± 0.033 a	$1648 \pm 450ab$	$1305 \pm 227ab$
N600	$163.75 \pm 16.53b$	$6.831 \pm 0.81a$	$0.042 \pm 0.0030a$	$0.21 \pm 0.012a$	$1901 \pm 423b$	$1386\pm214b$

morphology. Root vitality is of utmost importance to identify the ability of plant roots to uptake water and nutrient as well as to determine root longevity (Rewald and Meinen, 2013). A previous study also found that fire-derived charcoal mass was positively correlated with root vitality for overstorey vegetation in a Gmelin larch forest (Bryanin and Makoto, 2017). These results indicate that nano-BC prepared at higher temperatures could more greatly reduce the negative effect of Cd²⁺ on rice plant growth relative to that of lower temperatures and bulk BC, which is probably ascribed to its smaller size and unique physicochemical properties (Xu et al., 2017). The size effect of N600 is evident when compared with B600 as shown in Fig. 1 and Table 2. The high dispersibility and surface reactivity make N600 more easily attach to and interact with the root surface of rice plants, which may be beneficial for Cd²⁺ immobilization and physical protection for the roots.

3.3. Biochemical and physiological responses of rice plants

When subjected to stress, plants respond mainly through alteration in biochemical and physiological processes. The presence of nano-BC probably mitigated the physiological damage of Cd^{2+} to rice plants as reflected by the changes of chlorophyll and MDA contents, as well as relative electrical conductivity of leaves (Fig. 2). It is reported that 5.0 mg/L Cd^{2+} in aqueous solutions could greatly decrease the chlorophyll content of rice seedlings (Guo et al., 2018), consistent with the result when only treated with Cd^{2+} in this study. However, the contents of chlorophyll a and b, and total chlorophyll were significantly enhanced by BC addition, which followed the same order of rice growth as mentioned above (Fig. 2a). For MDA content and relative electrical conductivity, they were decreased by the application of nano-BC (Fig. 2b and c). MDA content is generally used as an index of lipid peroxidation under

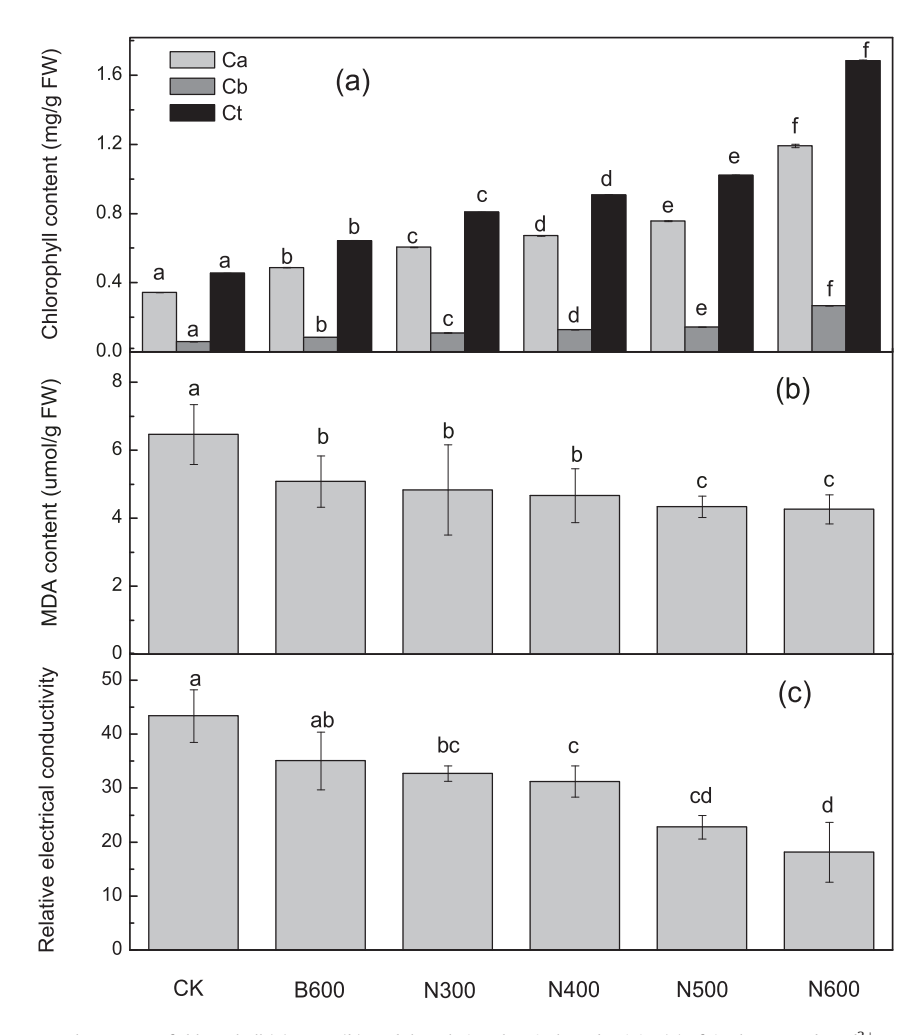


Fig. 2. Effects of bulk- and nano-BCs on the content of chlorophyll (a), MDA (b), and the relative electrical conductivity (c) of rice leaves under Cd^{2+} stress (5.0 mg/L for 7 days). Different letters represent different statistical groups suggested by the Tukey-HSD multiple comparisons at p < 0.05.

stressful conditions. The gradually decreased MDA level (Fig. 2b) indicates that oxidative damage in rice plants induced by Cd²⁺ treatment was alleviated by BC. Membrane permeability of leaves, reflected by relative electrical conductivity, is an important indicator for cellular damage of plants, which is also reduced due to the addition of BC (Fig. 2c). Compared with bulk BC (i.e., B600), nano-BC, especially the higher-temperature ones, more greatly alleviated Cd stress and toxicity to rice seedlings.

Additionally, enzymatic antioxidant systems including SOD, POD, and CAT played a crucial role in scavenging harmful oxygen species. The impact of nano-BC on antioxidative enzyme activities in rice leaves and roots under Cd stress is shown in Fig. 3(a-c). It is well known that exposure of heavy metals with relatively high concentrations could lead to the enhancement of antioxidative enzyme activity due to oxidative stress (Nadgorska-Socha et al., 2013). Consistently, the activities of SOD, POD, and CAT after treated by 5.0 mg/L Cd²⁺ in this study were higher than the data in the literature treated with lower concentrations of Cd²⁺ (Guo et al., 2007). However, it was unexpected that the addition of nano-BC further increased the activities of SOD, POD, and CAT compared with the control only treated with Cd²⁺ ions, which indicates that nano-BC could modulate the oxidative stress in the rice plants, Similarly, the content of soluble protein in both leaves and roots was greatly increased by the addition of high-temperature nano-BC (N500 and N600) (Fig. 3d). By contrast, the bulk BC particles (B600) had little effect on the variations of enzyme activities and soluble protein content. Relative to bulk BC, it is more easily for nano-BC to attach (or deposit) onto the root surfaces of rice plants and directly contact with the roots, which was confirmed by the observation that a plenty of nano-BC particles were tightly adhered to the root surfaces and could not be removed by thoroughly washing with water. It is reported that free radicals can be generated during charring and then stored in the BC particles for hours, days (Lomnicki et al., 2008), and even months (Liao et al., 2014). With the presence of free radicals, the suspension of BC materials in aqueous solutions may induce reactive oxygen species (ROS) generation (Fang et al., 2015), which probably stimulates the antioxidative system of the plants to mitigate the oxidative damage. As shown in Fig. 4, EPR signals were observed for both the nano- and bulk-BCs, where the signal intensity followed the order of B600 > N600 > N500 > N400 > N300 and correlated with the enhancement of antioxidative enzyme activities except for B600. Liao et al. found that the free radicals in BC caused significant germination inhibition and growth retardation for corn, wheat, and rice seedlings (Liao et al., 2014). However, the authors did not examine the responses of antioxidative system to free radicals. Furthermore, the experiment in that study was carried out in Petri dishes with 90 mm diameter and thus the bulk BC particles had easy contact with plant roots. To reflect the real environment more closely, we employed hydroponic culture in the present study where we noticed that the bulk BC settled down completely in a short time and had less opportunity to contact with the roots; while the high dispersibility of nano-BC allowed for many more chances to interact with the roots. This might greatly reduce the impact of B600 on the changes of antioxidative enzyme activities. Besides free radicals, the phytotoxic compounds and/or heavy metals derived from BC (if any) could also negatively affect the plant growth (Rogovska et al., 2012). However, few metal/metalloid elements and polycyclic aromatic hydrocarbons were detected from the leachates of BC used in this study (data not shown) using the previously reported extraction methods (Qiu et al., 2015). These results remind us of the possible physiological damage of free radicals derived from nano-BC on plant growth, which merits further study in the future.

3.4. Uptake of Cd by rice plants

The Cd contents in plant tissues significantly decreased by the addition of nano-BC and negatively correlated with the charring temperature (Fig. 5), indicating that nano-BC with higher temperatures was

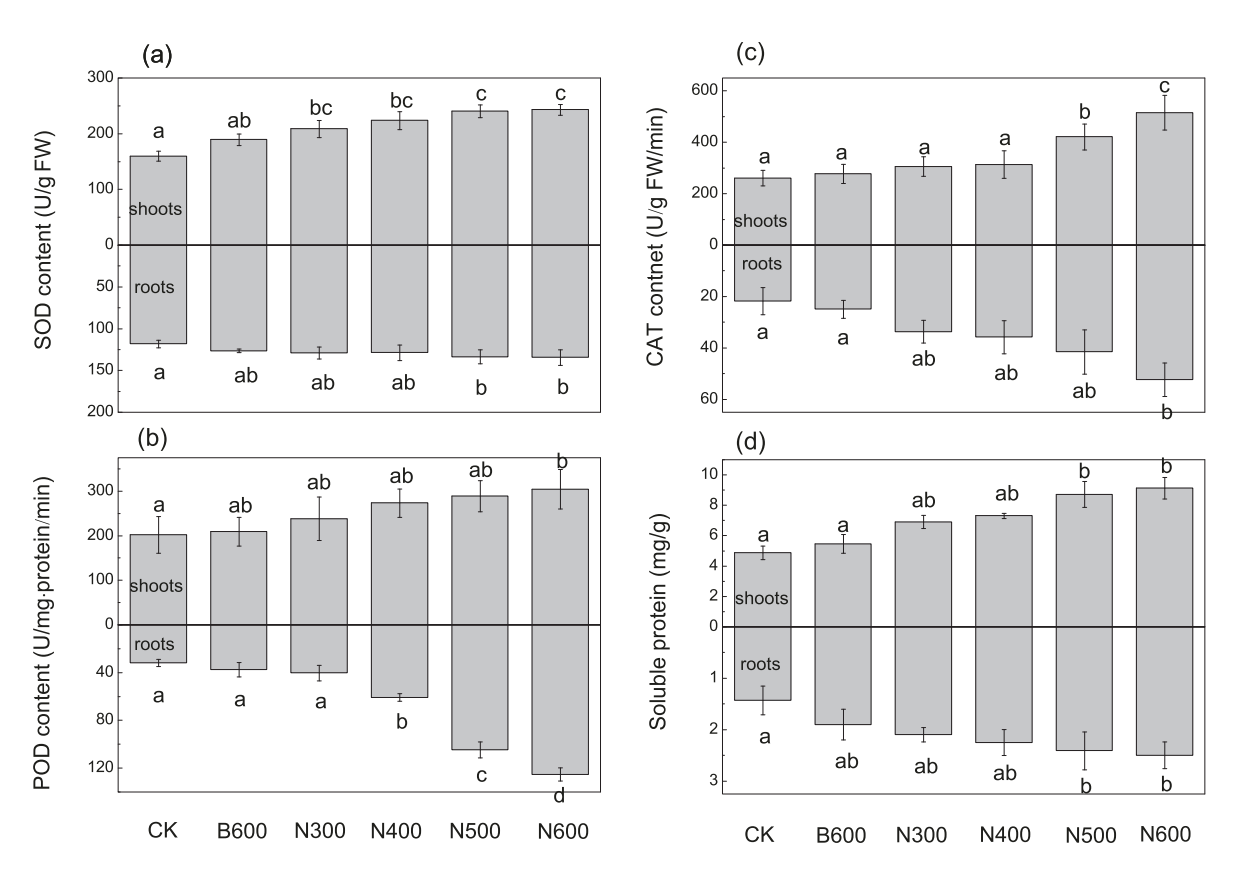


Fig. 3. Bulk- and nano-BCs elevated the contents of protective enzymes (a–c) and soluble protein (d) of rice plants after Cd^{2+} exposure (5.0 mg/L) for 7 days. Different letters represent different statistical groups suggested by the Tukey-HSD multiple comparisons at p < 0.05.

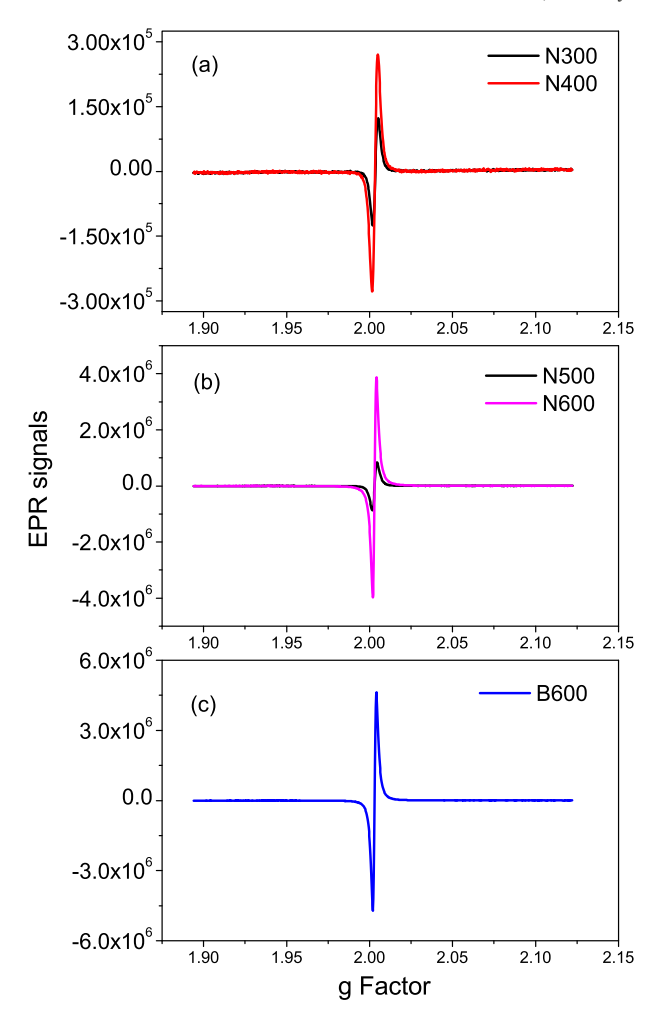


Fig. 4. EPR measurement of nano-BC (N300-N600) and bulk BC (B600).

more efficient in reducing the accumulation of Cd by rice plants. Comparatively, the uptake of Cd was also greatly inhibited by the presence of B600, but its effect was significantly lower than that of N500 and N600. Taking a closer look, N500 and N600 had similar effect on reducing the Cd uptake of plants, which was much higher than other treatments. We hypothesize that the higher capacity of N500 and N600 for immobilizing Cd may be related to their high adsorption capacities for Cd²⁺. Thus, adsorption of Cd²⁺ on bulk BC (i.e., B300-B600) and nano-

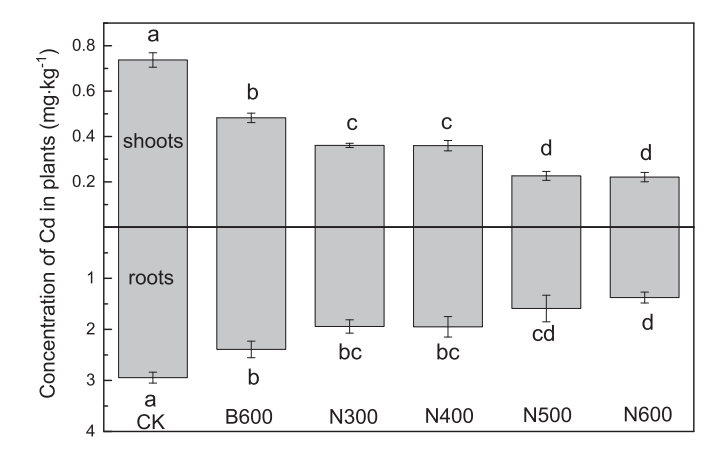


Fig. 5. Cd uptake in the shoots and roots of rice plants with the treatments of only Cd^{2+} (CK) and Cd^{2+} with the presence of BC. Different letters represent different statistical groups suggested by the Tukey-HSD multiple comparisons at p < 0.05.

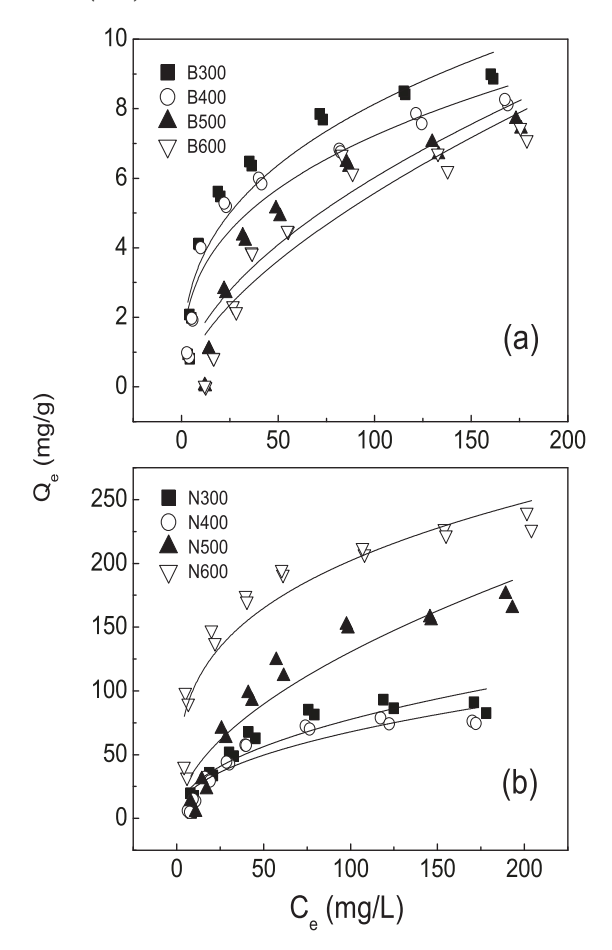


Fig. 6. Adsorption isotherms of Cd^{2+} on the bulk- and nano-BCs (i.e., B300-B600 and N300-N600), respectively, showing the higher adsorption on the nano-BC.

BC (i.e., N300-N600) was carried out simultaneously to directly compare their binding affinities (Fig. 6). The data were fitted with the Freundlich model ($Q = K_f C_e^n$), where Q is the solid-phase concentration of Cd^{2+} (mg/g), C_e is the liquid-phase concentration of the solute (mg/L), K_f is the Freundlich affinity coefficient ((mg/g)/(mg/L)ⁿ), and n (unitless) is the Freundlich linearity index. The Freundlich model fitting parameters are listed in Table 3.

It is evident that nano-BC exhibited much higher adsorption for ${\rm Cd}^2$ + than bulk-BC. Their adsorption affinities were compared by distribution coefficient ($K_{\rm d}=Q/C_{\rm e},$ L/g) when the aqueous concentration of ${\rm Cd}^{2+}$ was 5.0 mg/L. The $K_{\rm d}$ values of nano-BC were around 10–100 times higher than those of bulk-BC. The higher adsorption affinity of nano-BC is mainly attributed to its large surface area, numerous oxyl groups and mineral constituents (Shen et al., 2015). Considering the high colloidal stability and surface reactivity, it is reasonable to believe that nano-BC would play a more important role in biogeochemical

Table 3 Freundlich model parameters of Cd^{2+} adsorption on the bulk- and nano-BCs (i.e., B300-B600 and N300-N600), respectively.

ВС	$K_{\rm F}\left(({\rm mg/g})/({\rm mg/L})^n\right)$	n	R^2	$K_{\rm d} ({\rm L/g}) (C_{\rm e} = 5.0 {\rm mg/L})$
B300	1.622	0.350	0.893	0.570
B400	1.492	0.343	0.904	0.518
B500	0.462	0.558	0.849	0.227
B600	0.322	0.620	0.854	0.175
N300	9.197	0.464	0.839	3.881
N400	8.531	0.451	0.845	3.526
N500	10.77	0.542	0.889	5.153
N600	52.45	0.293	0.880	16.81

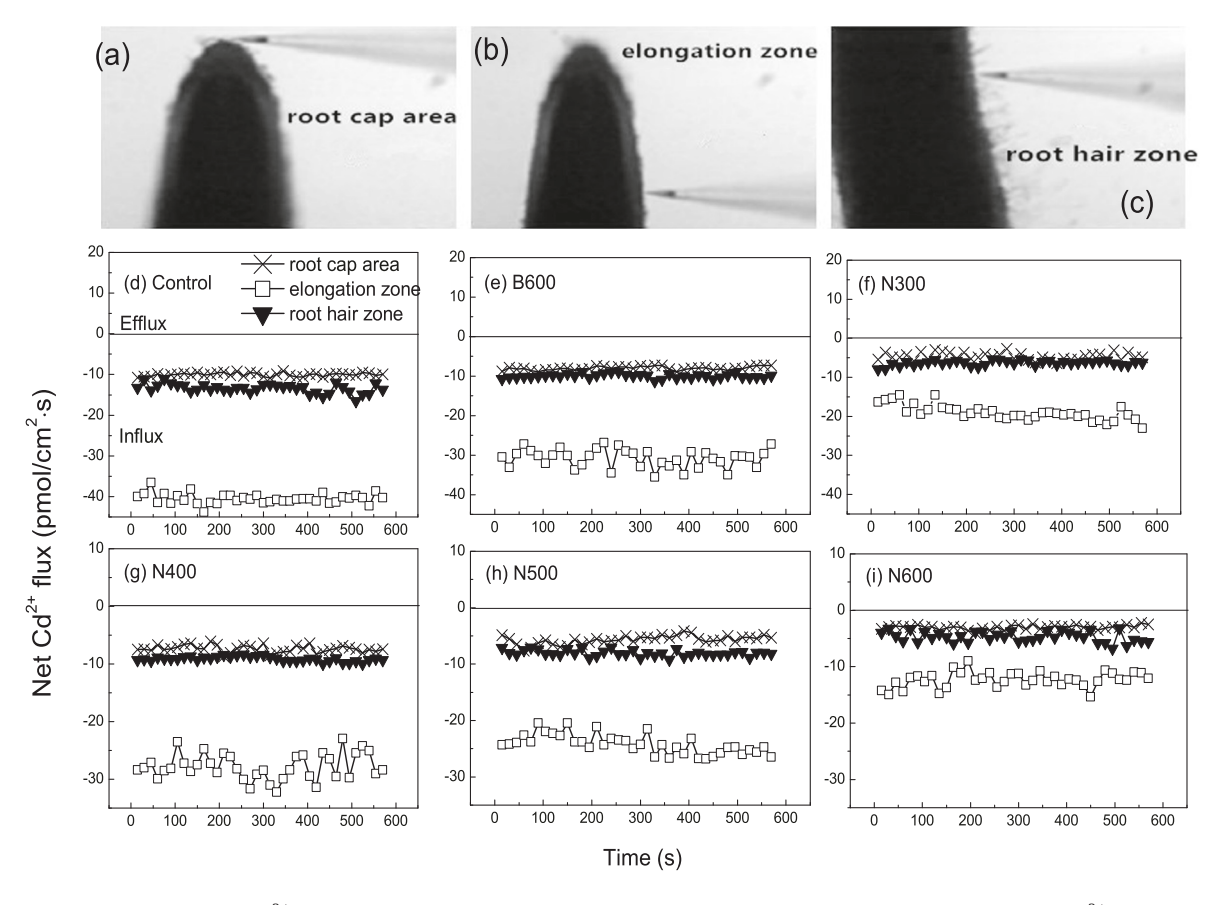
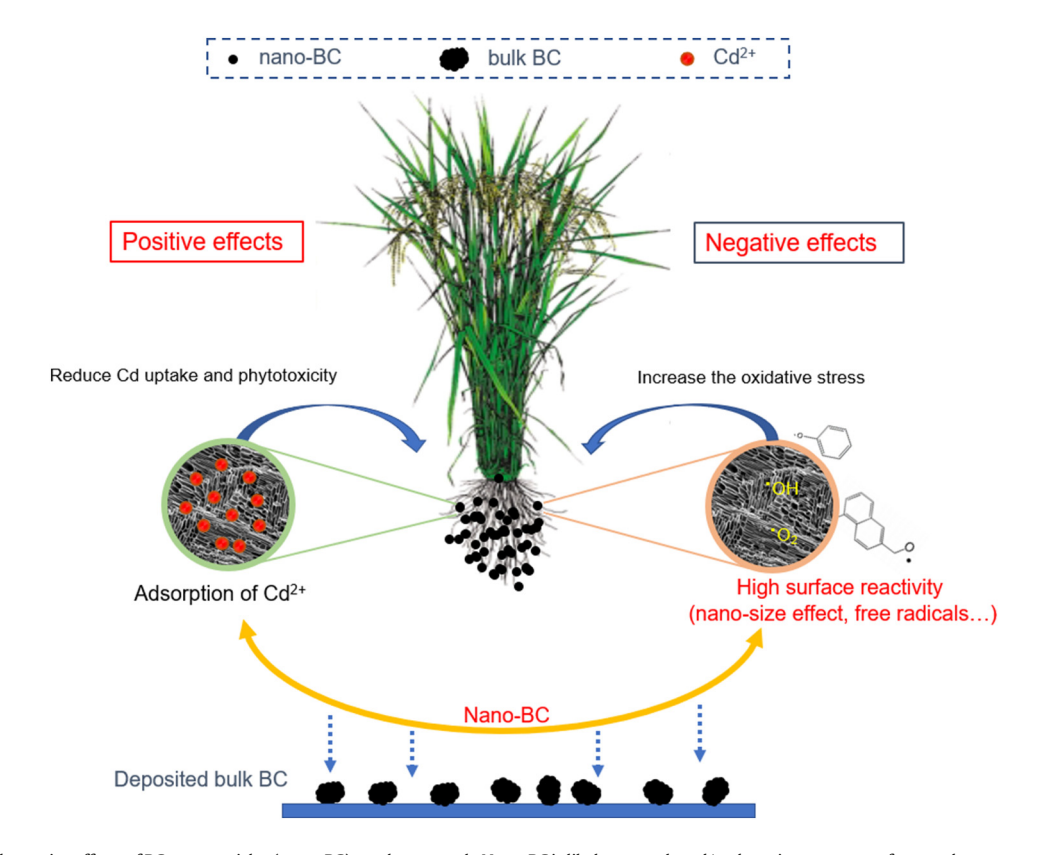


Fig. 7. Effect of BC particles on the kinetics of Cd^{2+} flux in the elongation zone, root hair zone, and root cap area, respectively, with the presence of 5.0 mg/L Cd^{2+} in the measuring medium determined by the scanning ion-selective electrode technique (SIET).



Scheme 1. Positive and negative effects of BC nanoparticles (nano-BC) on plant growth. Nano-BC is likely to attach and/or deposit onto root surfaces and more greatly inhibits the uptake of Cd²⁺ by the plants relative to bulk BC. Meanwhile, the high surface reactivity of nano-BC may induce oxidative stresses to the plants.

processes in the water and soil environments than bulk BC. More remarkably, distinct adsorption patterns were observed between bulkand nano-BCs. For bulk-BC, the low-temperature BCs (i.e., B300 and B400) had higher adsorption of Cd²⁺ than the high-temperature ones (i.e., B500 and B600). The result is consistent with many previous studies (Dong et al., 2013; Uchimiya et al., 2011; Zhang et al., 2015). Adsorption of heavy metals is mainly driven by a number of molecular interactions between functional groups of BC and heavy metals such as ion-exchange and surface complexation (Lian and Xing, 2017). Thus, the adsorption affinity of heavy metals is more dependent on the surface chemistry of BC than surface area and pore volume. With increasing pyrolytic temperature, a majority of functional groups on BC were gradually decomposed, leading to the decreased adsorption of heavy metals on high-temperature BC (Zhang et al., 2015). For nano-BC, however, the opposite was observed, i.e., the high-temperature nano-BC had higher adsorption affinity for Cd2+ than the lowtemperature ones (Fig. 6), which is probably due to its nanometer size and plenty of surficial oxyl groups as mentioned above. Similarly, adsorption of Cr³⁺ on BC with a particle size < 2.0 µm was two to three times greater than that on bulk BC; and, the adsorption was enhanced by increasing pyrolytic temperature for the smaller size BC particles (Qian et al., 2016). These results indicate that the effect of charring temperature on the property of nano-BC is very different from that of bulk BC due to their distinct forming mechanisms. Overall, it can be concluded that the higher adsorption affinity of nano-BC for Cd²⁺ contributes greatly to the decreased uptake of Cd by rice plants with the presence of N500 or N600. Meanwhile, the positive impact of nano-BC to reduce Cd uptake significantly offsets its growth inhibition to rice plants.

3.5. Net fluxes of Cd^{2+} in the roots of rice plants

To more directly demonstrate the effect of nano-BC on reducing the uptake of Cd^{2+} by plant roots, the kinetics of Cd^{2+} fluxes in the elongation zone, root hair zone, and root cap area in the presence and absence of BC particles were measured by SIET, respectively (Fig. 7). It is evident that Cd^{2+} net influx in the elongation zone was much higher than that of root hair and cap areas and remained relatively constant in the tested period (10 min) after exposure to 5.0 mg/L Cd^{2+} , indicating that the elongation zone might be one of the most important regions of rice roots to absorb Cd^{2+} . Similarly, Li et al. observed that the elongation zone was the major uptake location of Cd^{2+} for the root of halophyte *Suaeda salsa* (Li et al., 2012). Also, it was found that the influx of Cd^{2+} measured 1 and 2 mm back from the root apex was 4 times higher than that measured further back from the root apex in the root tip of wheat (*Triticum aestivum* L.) (Pineros et al., 1998).

The Cd²⁺ net influx of different root zones responded distinctly to the presence of BC particles (Fig. 7d-i). It can be seen that BC particles including nano-BC had little effect on reducing Cd²⁺ influx for the root hair and cap areas, however, they significantly inhibited Cd²⁺ influx for the elongation zone. For example, the mean values of Cd²⁺ net influxes in both root hair and cap zones remained at ca. 10 pmol/cm²·s for all the treatments, by contrast, those in the elongation zone decreased from ca. 40 pmol/cm²·s in the absence of BC to 12 pmol/cm²·s when N600 was added. The result clearly demonstrated that the attached or deposited nano-BC on root surfaces greatly reduced the amount of Cd²⁺ entering root epidermal cells due to its high adsorption affinity for Cd²⁺ as mentioned above. Thus, we inferred that a shelllike structure might be formed on the surfaces of root tips due to the attachment of nano-BC, which effectively reduced the uptake of Cd²⁺ by rice plants. However, the shell-like structure is not uniformly distributed on the root surfaces as observed in this study, which is probably attributed to the different interactions between nano-BC and various root regions and/or root exudates.

Based on the above analysis, a scheme was proposed to illustrate the positive and negative effects of nano-BC on the growth of rice plants

under the exposure of heavy metals (Scheme 1). After entering into the rhizosphere, nano-BC could suspend well in the aqueous solution due to its high colloidal stability, hence, a large number of nano-BC would contact with and then attach (or deposit) to the surface of plant roots. By contrast, the bulk BC particles might settle down quickly and have much less opportunity to make contact with the roots. The attached nano-BC has a very high adsorption affinity for Cd²⁺ (at least 10 times higher than that of the bulk BC), which could greatly inhibit Cd uptake into plant roots and thus reduce its phytotoxicity. However, the free radical induced high surface reactivity is likely to alter the rhizosphere environment or directly stimulate the plants to generate stress responses such as the enhancement of antioxidative enzyme activity in this study, which would be highly dependent on the plant species as well as concentration and properties of nano-BC. Therefore, the potential risk of BC materials on plant growth deserves further investigation in the future.

4. Environmental implications

Relative to bulk BC particles, nano-BC is more active and expected to participate in a larger number of biogeochemical processes in the environment. The results in this study indicate that a higher charring temperature is more favorable to the formation of nano-BC. The hightemperature nano-BC exhibited more developed pore structure and higher Si content than the low-temperature one, indicating higher surface reactivity. Consistently, both N500 and N600 are more efficient in alleviating the phytotoxicity of Cd²⁺ in rice plants based on the basis of plant growth, biochemical responses, and Cd uptake. It is foreseeable that a number of nano-BC particles could attach (or deposit) onto root surfaces and probably form a shell-like structure, which greatly inhibits Cd²⁺ net influx to root cells due to its high adsorption affinity for Cd²⁺ in the aqueous solution. However, it is still not clear how and to what extent the nano-BC interacts with root surfaces (or root exudates) leading to the attachment and deposition of nano-BC. On the other hand, not only positive but also adverse effects of nano-BC were found in this study. The enhanced antioxidative enzyme activities of rice plants in the presence of nano-BC indicate that nano-BC might induce oxidative stress owing to its unique properties such as the presence of free radicals. However, the real soil environment is much more complicated than the hydroponic condition used in the present study, and therefore the observations need to be further verified in the soil matrix. We call for investigative attention to the molecular interactions between nano-BC and root epidermal cells as well as root exudates in the rhizosphere environment with special attention to the emerging properties of nano-BC including the generation of persistent free radicals and its redox characteristics. These results are crucial for better understanding the efficiency of BC amendment in plant growth and the bioavailability of pollutants.

Acknowledgements

The authors gratefully acknowledge financial support from the National Natural Science Foundation of China (41573127), the National Key Research and Development Program (2016YFD0800201), China Scholarship Council (201503250054) for F.L. to study at UMass Amherst, USDA McIntire-Stennis Program (MAS 00028), and NSF (CBET 1739884).

Appendix A. Supplementary data

Supplementary data to this article can be found online at https://doi.org/10.1016/j.scitotenv.2018.11.364.

References

Archanjo, B.S., Mendoza, M.E., Albu, M., Mitchell, D.R.G., Hagemann, N., Mayrhofer, C., et al., 2017. Nanoscale analyses of the surface structure and composition of biochars extracted from field trials or after co-composting using advanced analytical electron microscopy. Geoderma 294. 70–79.

- Bryanin, S.V., Makoto, K., 2017. Fire-derived charcoal affects fine root vitality in a post-fire Gmelin larch forest; field evidence. Plant Soil 416, 409–418.
- Dong, X., Ma, L.Q., Zhu, Y., Li, Y., Gu, B., 2013. Mechanistic investigation of mercury sorption by Brazilian pepper biochars of different pyrolytic temperatures based on X-ray photoelectron spectroscopy and flow calorimetry. Environ. Sci. Technol. 47, 12156–12164.
- Du, Y., Zhu, L., Shan, G., 2012. Removal of Cd²⁺ from contaminated water by nano-sized aragonite mollusk shell and the competition of coexisting metal ions. J. Colloid Interface Sci. 367, 378–382.
- Fang, G., Zhu, C., Dionysiou, D.D., Gao, J., Zhou, D., 2015. Mechanism of hydroxyl radical generation from biochar suspensions: implications to diethyl phthalate degradation. Bioresour. Technol. 176, 210–217.
- Guo, B., Liang, Y.C., Zhu, Y.G., Zhao, F.J., 2007. Role of salicylic acid in alleviating oxidative damage in rice roots (*Oryza sativa*) subjected to cadmium stress. Environ. Pollut. 147, 743–749
- Guo, L., Chen, A., He, N., Yang, D., Liu, M., 2018. Exogenous silicon alleviates cadmium toxicity in rice seedlings in relation to Cd distribution and ultrastructure changes. J. Soils Sediments 18. 1691–1700.
- Khan, S., Cai, C., Waqas, M., Arp, H.P., Zhu, Y.G., 2013. Sewage sludge biochar influence upon rice (*Oryza sativa* L) yield, metal bioaccumulation and greenhouse gas emissions from acidic paddy soil. Environ. Sci. Technol. 47, 8624–8632.
- Klüpfel, L., Keiluweit, M., Kleber, M., Sander, M., 2014. Redox properties of plant biomassderived black carbon (biochar). Environ. Sci. Technol. 48, 5601–5611.
- Li, L., Liu, X., Peijnenburg, W.J.G.M., Zhao, J., Chen, X., Yu, J., et al., 2012. Pathways of cadmium fluxes in the root of the halophyte Suaeda salsa. Ecotoxicol. Environ. Saf. 75
- Lian, F., Xing, B., 2017. Black carbon (biochar) in water/soil environments: molecular structure, sorption, stability, and potential risk. Environ. Sci. Technol. 51, 13517–13532.
- Liao, S., Pan, B., Li, H., Zhang, D., Xing, B., 2014. Detecting free radicals in biochars and determining their ability to inhibit the germination and growth of corn, wheat and rice seedlings. Environ. Sci. Technol. 48, 8581–8587.
- Lindström, A., Nyström, C., 1987. Seasonal variation in root hardiness of container-grown Scots pine, Norway spruce, and lodgepole pine seedlings. Can. J. For. Res. 17, 787–793.
- Liu, G.C., Zheng, H., Jiang, Z.X., Zhao, J., Wang, Z.Y., Pan, B., Xing, B.S., 2018. Formation and physicochemical characteristics of nano biochar: insight into chemical and colloidal stability. Environ. Sci. Technol. 52, 10369–10379.
- Lomnicki, S., Truong, H., Vejerano, E., Dellinger, B., 2008. Copper oxide-based model of persistent free radical formation on combustion-derived particulate matter. Environ. Sci. Technol. 42, 4982–4988.
- Major, J., Lehmann, J., Rondon, M., Goodale, C., 2010. Fate of soil-applied black carbon: downward migration, leaching and soil respiration. Glob. Chang. Biol. 16, 1366–1379.
- Marion, B.M., 1976. A rapid and sensitive method for the quantitation of microgram quantities of protein utilizing the principle of protein-dye binding. Annu. Rev. Biochem. 72, 248–254.
- Nadgorska-Socha, A., Kafel, A., Kandziora-Ciupa, M., Gospodarek, J., Zawisza-Raszka, A., 2013. Accumulation of heavy metals and antioxidant responses in *Vicia faba* plants grown on monometallic contaminated soil. Environ. Sci. Pollut. Res. 20, 1124–1134.
- Pignatello, J.J., Kwon, S., Lu, Y., 2006. Effect of natural organic substances on the surface and adsorptive properties of environmental black carbon (char): attenuation of surface activity by humic and fulvic acids. Environ. Sci. Technol. 40, 7757–7763.
- Pignatello, J.J., Mitch, W.A., Xu, W., 2017. Activity and reactivity of pyrogenic carbonaceous matter toward organic compounds. Environ. Sci. Technol. 51, 8893–8908.
- Pineros, M.A., Shaff, J.E., Kochian, V., 1998. Development, characterization, and application of a cadmium-selective microelectrode for the measurement of cadmium fluxes in roots of Thlaspi species and wheat. Plant Physiol. 116, 1393–1401.
- Qian, L.B., Zhang, W.Y., Yan, J.C., Han, L., Gao, W.C., Liu, R.Q., et al., 2016. Effective removal of heavy metal by biochar colloids under different pyrolysis temperatures. Bioresour. Technol. 206, 217–224.
- Qiu, Y., Xiao, X., Cheng, H., Zhou, Z., Sheng, G.D., 2009. Influence of environmental factors on pesticide adsorption by black carbon: pH and model dissolved organic matter. Environ. Sci. Technol. 43, 4973–4978.
- Qiu, M.Y., Sun, K., Jin, J., Han, L.F., Sun, H.R., Zhao, Y., et al., 2015. Metal/metalloid elements and polycyclic aromatic hydrocarbon in various biochars: the effect of feedstock, temperature, minerals, and properties. Environ. Pollut. 206, 298–305.
- Qu, X., Fu, H., Mao, J., Ran, Y., Zhang, D., Zhu, D., 2016. Chemical and structural properties of dissolved black carbon released from biochars. Carbon 96, 759–767.

- Rewald, B., Meinen, C., 2013. Plant roots and spectroscopic methods analyzing species, biomass, and vitality. Front. Plant Sci. 4, 1–9.
- Rico, C.M., Hong, J., Morales, M.I., Zhao, L., Barrios, A.C., Zhang, J.-Y., et al., 2013. Effect of cerium oxide nanoparticles on rice: a study involving the antioxidant defense system and in vivo fluorescence imaging. Environ. Sci. Technol. 47, 5635–5642.
- Rogovska, N., Laird, D., Cruse, R.M., Trabue, S., Heaton, E., 2012. Germination tests for assessing biochar quality. J. Environ. Qual. 41, 1014–1022.
- Shah, K., Kumar, R.G., Verma, S., Dubey, R.S., 2001. Effect of cadmium on lipid peroxidation, superoxide anion generation and activities of antioxidant enzymes in growing rice seedlings. Plant Sci. 161, 1135–1144.
- Shen, Z.T., Jin, F., Wang, F., McMillan, O., Al-Tabbaa, A., 2015. Sorption of lead by Salisbury biochar produced from British broadleaf hardwood. Bioresour. Technol. 193, 553–556.
- Silber, A., Levkovitch, I., Graber, E.R., 2010. pH-dependent mineral release and surface properties of cornstraw biochar: agronomic implications. Environ. Sci. Technol. 44, 9318–9323
- Singh, B.P., Cowie, A.L., Smernik, R.J., 2012. Biochar carbon stability in a clayey soil as a function of feedstock and pyrolysis temperature. Environ. Sci. Technol. 46, 11770–11778
- Song, Y., Wang, F., Kengara, F.O., Yang, X., Gu, C., Jiang, X., 2013. Immobilization of chlorobenzenes in soil using wheat straw biochar. J. Agric. Food Chem. 61, 4210–4217.
- Spokas, K.A., Novak, J.M., Masiello, C.A., Johnson, M.G., Colosky, E.C., Ippolito, J.A., et al., 2014. Physical disintegration of biochar: an overlooked process. Environ. Sci. Technol. Lett. 1, 326–332.
- Sun, J., Wang, R., Liu, Z., Ding, Y., Li, T., 2013. Non-invasive microelectrode cadmium flux measurements reveal the spatial characteristics and real-time kinetics of cadmium transport in hyperaccumulator and nonhyperaccumulator ecotypes of *Sedum alfredii*. J. Plant Physiol. 170, 355–359.
- Sun, J., Lian, F., Liu, Z., Zhu, L., Song, Z., 2014. Biochars derived from various crop straws: characterization and Cd(II) removal potential. Ecotoxicol. Environ. Saf. 106, 226–231.
- Uchimiya, M., Wartelle, L.H., Klasson, K.T., Fortier, C.A., Lima, I.M., 2011. Influence of pyrolysis temperature on biochar property and function as a heavy metal sorbent in soil. J. Agric. Food Chem. 59, 2501–2510.
- Van Zwieten, L., Kimber, S., Morris, S., Chan, K.Y., Downie, A., Rust, J., et al., 2010. Effects of biochar from slow pyrolysis of papermill waste on agronomic performance and soil fertility. Plant Soil 327, 235–246.
- Wang, D., Zhang, W., Hao, X., Zhou, D., 2012. Transport of biochar particles in saturated granular media: effects of pyrolysis temperature and particle size. Environ. Sci. Technol. 47, 821–828.
- Weng, Z., Van Zwieten, L., Singh, B.P., Tavakkoli, E., Joseph, S., Macdonald, L.M., et al., 2017.
 Biochar built soil carbon over a decade by stabilizing rhizodeposits. Nat. Clim. Chang. 7. 371–376.
- Xu, F., Wei, C., Zeng, Q., Li, X., Alvarez, P.J.J., Li, Q., et al., 2017. Aggregation behavior of dissolved black carbon: implications for vertical mass flux and fractionation in aquatic systems. Environ. Sci. Technol. 51, 13723–13732.
- Yang, J., Pan, B., Li, H., Liao, S., Zhang, D., Wu, M., et al., 2016. Degradation of p-nitrophenol on biochars: role of persistent free radicals. Environ. Sci. Technol. 50, 694–700.
- Yi, P., Pignatello, J.J., Uchimiya, M., White, J.C., 2015. Heteroaggregation of cerium oxide nanoparticles and nanoparticles of pyrolyzed biomass. Environ. Sci. Technol. 49, 13294–13303.
- Zhang, H.J., Zhang, N., Yang, R.C., Wang, L., Sun, Q.Q., Li, D.B., et al., 2014. Melatonin promotes seed germination under high salinity by regulating antioxidant systems, ABA and GA(4) interaction in cucumber (*Cucumis sativus L.*). J. Pineal Res. 57, 269–279.
- Zhang, F., Wang, X., Yin, D.X., Peng, B., Tan, C.Y., Liu, Y.G., et al., 2015. Efficiency and mechanisms of Cd removal from aqueous solution by biochar derived from water hyacinth (*Eichornia crassipes*). J. Environ. Manag. 153, 68–73.
- Zhao, L., Cao, X.D., Masek, O., Zimmerman, A., 2013. Heterogeneity of biochar properties as a function of feedstock sources and production temperatures. J. Hazard. Mater. 256, 1.0
- Zhao, Y., Zhang, S., Wen, N., Zhang, C., Wang, J., Liu, Z., 2017. Modeling uptake of cadmium from solution outside of root to cell wall of shoot in rice seedling. Plant Growth Regul. 82, 11–20.